

## EQUAL AREA METHOD TO OBTAIN APPROXIMATE SOLUTION OF ADSORPTION RATE MODEL WITH NONLINEAR ISOTHERM

Dong Kwon KEUM and Won Kook LEE\*

Department of Chemical Engineering, Korea Advanced Institute of Science and Technology,  
P.O. Box 131, Cheongryang, Seoul 130-650, Korea

(Received 31 December 1987 • accepted 24 June 1988)

---

**Abstract**—Intraparticle mass transfer coefficients were determined by experimental adsorption data of *m*-cresol, quinoline and 1-naphthol onto a silica gel in a finite bath. The equal area approximation method of nonlinear isotherm was proposed with the assumption that the internal mass transfer coefficient is constant and equal to average value in the operating region. In the region where a slope of a constant time line is less than that of the operating line (region I), the original nonlinear isotherm was approximated by a quadratic form, and in the inverse case (region II) the isotherm was approximated by a linear form. Thus approximate analytical solutions were obtained. The present experimental conditions were in the region II, and the present approximate solution was in a good agreement with experimental results.

---

### INTRODUCTION

Design and scale up of adsorption equipments require informations on the equilibrium relation and the rate parameters which represent mass transfer effects such as film diffusion and intraparticle mass transfer. The value of the film mass transfer coefficient can be estimated from the correlation equations in the literatures. It is also known that the batch experiment with a proper model equation for diffusion into the particles is an effective method to obtain value of the intraparticle mass transfer coefficients [1,2].

For expressing the intraparticle mass transfer rates Fick's second law was applied by many investigators [3-9]. But for engineering applications it is useful to express the rate equation for intraparticle mass transfer in terms of a certain explicit function of the average concentration instead of the point concentration. Glueckauf and Coates [10] assumed that the rate of mass transfer into the particles is proportional to the difference between the average concentration of the solute in the particle and the surface concentration of the particle in equilibrium with the fluid phase. The validity of their assumption was subsequently supported by Jury [11]. It is so called as "Glueckauf's linear driving force approximation model", and this model was also used in the many literatures [2,12,13].

If the equilibrium relation is linear, the solution to model equation is analytically obtained. But the equi-

librium relations of the liquid adsorption was known to be nonlinear in the most cases, and thus numerical technique was commonly required for the solution. To overcome this difficulty, Tien [8] and Miller & Clump [13] obtained the analytical solution with assumption that the concentration of the fluid phase at the particle surface is a function of time in a polynomial form. Also Spahn and Schlünder [2] had obtained the analytical solution of a model equation for the system which has highly favorable type of isotherm with assumption of the hypothetical constant equilibrium concentration. Another method for obtaining analytical solution had been conceptually initiated by Dryden and Kay [14], and subsequently attempted by Hashimoto et al. [4]. The basic idea of their method was to transform of the original nonlinear isotherm to a simplified form which can be used to obtain the analytical solution. But their methods did not have any theoretical basis and also had some limitation in selection of the operating conditions to be used in the solution with reasonable accuracy.

The purposes of the present work are to obtain the analytical solution of the model equation by approximating the original nonlinear isotherm, and to determine the intraparticle mass transfer coefficient from the analytical solution and experimental data.

### MATHEMATICAL MODEL

The liquid is perfectly mixed by suitable agitation so that the liquid concentration is uniform throughout

---

\*To whom all correspondence should be addressed.

the bath except a mass transfer boundary layer near the surface of each particle. Then an overall mass balance for a solute in the bath gives that

$$V(C - C_o) + Wq = 0 \quad (1)$$

where  $q$  is the average concentration in the solid phase and  $C_o$  is the initial concentration in the fluid phase.

To express the rate equation for diffusion into the particles, Glueckauf's linear driving force approximation model was applied. The mass transfer rate on unit volume with assumption of spherical particles are then described by the following relationship;

$$\rho_s \frac{dq}{dt} = \frac{3}{R} k_s \rho_p (q_s - q) \quad (2)$$

$$= \frac{3}{R} k_f (C - C_s) \quad (3)$$

where  $C_s$  and  $q_s$  are the concentration in the liquid and solid phase at the particle surface, respectively. Eqn(3) represents the mass transfer rate through the external surface film on the particles. Normally  $k_s$  is dependent on concentration [2], but it can be treated as a constant by taking as average value for the operating region. Since the rate of adsorption is much faster than that of the diffusion, the local equilibrium at the particle surface is maintained during the overall run time. Thus

$$q_s = q_s(C_s) \quad (4)$$

Initial conditions were

$$C = C_o, \quad q = 0 \quad (5)$$

From Eqn(2) and Eqn(3) the following relation was derived

$$q_s = q + \phi (C - C_s) \quad (6)$$

where  $\phi$  represents the relative importance of resistances in the external film and intraparticle phase, is equal to  $k_f/k_s \rho_p$ . The Eqn(1), Eqn(4), and Eqn(6) represent the operating line, the equilibrium curve, and the constant time line in Figure 1, and both slopes of Eqn(1) and Eqn(6) are constant throughout the experimental run with the assumption that system parameters are independent of time.

When a nonlinear isotherm is the favorable type as shown in Figure 1, the isotherm curve may be flattened with increasing concentration of the liquid phase, and then it is difficult for the programme to differentiate between any two values of the solid phase concentration and their corresponding  $C_s$  values as pointed out by McKay [12]. Under these conditions the program may go unstable. Although the difficulty can be avoided by reducing step size for integration, it requires much computation time. To overcome these deficiencies an analytical solution with approximation of the nonlinear isotherm would be more appropriate.

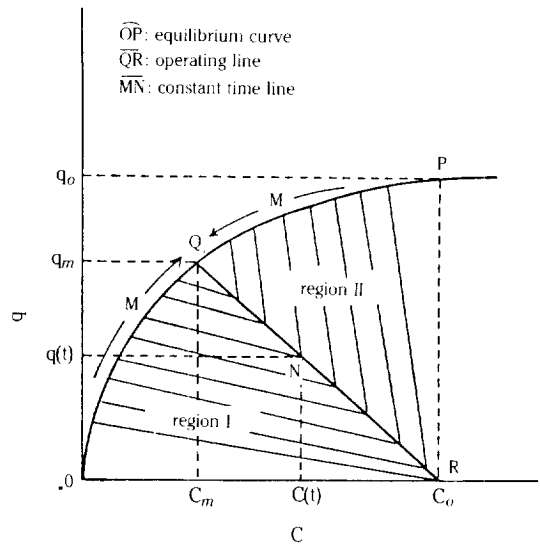


Fig. 1. Equilibrium curve, operating line and time constant line.

ated. This is the reason why the equal area approximate method was introduced. The approximation of the nonlinear isotherm was taken by different formula at each region as shown in Figure 2. The original isotherm may have large nonlinearity in region I while it may be nearly linear in region II. Although these aspects are not general, but it can be achieved by careful selection of operating conditions, i.e. by increasing the slope of the operating line. Thus the original nonlinear isotherm was approximated by a quadratic form in region I, and was approximated by a linear form in region II. Then the analytical solution can be obtained since  $q_s$  and  $C_s$  are explicitly expressed as a function of  $q$  and  $C$ . The approximate method of the each case was as follows;

### 1. Case of $\phi < V/W$ (region I)

The original isotherm, Eqn(4), was approximated by the following quadratic form

$$q_s^I = K_2^I C_s^2 + K_1^I C_s + K_0^I \quad (7)$$

and superscript I represents the region I. Eqn(7) is reduced to the linear form when  $K_2^I$  is zero, but it is not practical except dilute concentration region. Eqn(7) represents the dashed curve in Figure 2(a). For determining  $K_2^I$ ,  $K_1^I$  and  $K_0^I$ , the following three relations were exploited in present work.

$$i) \quad q_s^I(0) = q_s(0) = 0 \quad (8)$$

$$ii) \quad q_s^I(C_m) = q_s(C_m) = q_m \quad (9)$$

$$iii) \quad \int_0^{C_m} q_s^I dC_s = \int_0^{C_m} q_s dC_s \quad (\text{equal area}) \quad (10)$$

The first and second relation represented the condition

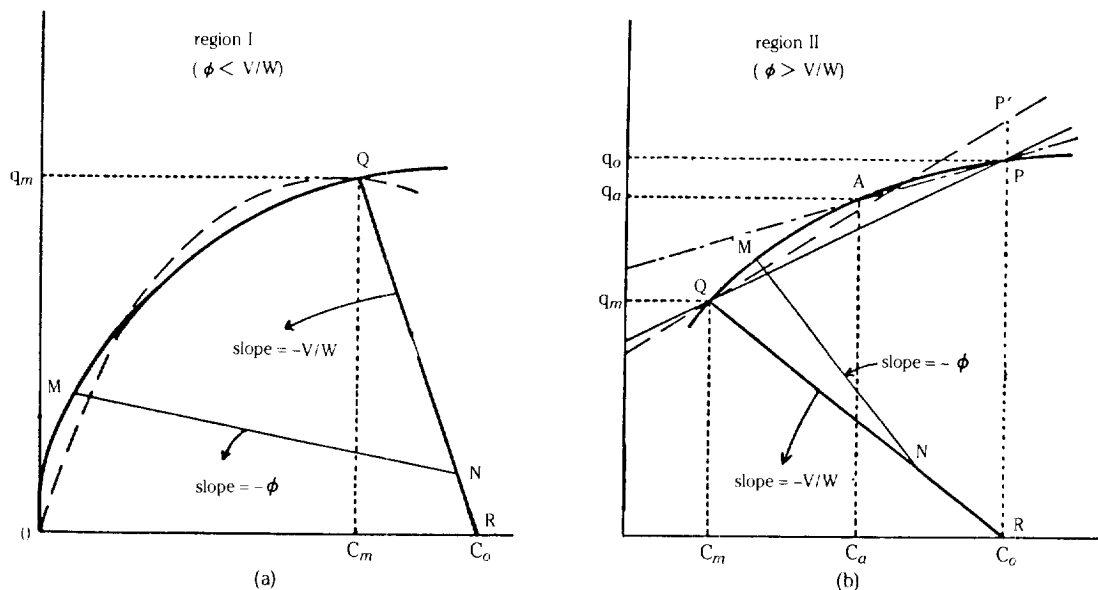


Fig. 2. Schematic diagram for approximation of the nonlinear isotherm.

which both the original isotherm and the approximated isotherm pass to points  $O(0,0)$  and  $Q(C_m, q_m)$  in Figure 2(a), and the third represented the assumption that the original isotherm and the approximated isotherm have same area under each isotherm in the region  $0 < C_s < C_m$ . The third relation was unique in this method and it may be theoretically reasonable than any other approximate method since the overall driving force by the original isotherm (solid curve) on Figure 2(a) are equal to that by the approximated isotherm (dashed curve) of Eqn(7). The following equation was derived from Eqn(7) to Eqn(10).

$$[K^I] = [A^I]^{-1} [B^I] \tag{11}$$

where

$$[K^I] = \begin{bmatrix} K_o^I \\ K_1^I \\ K_2^I \end{bmatrix}, [A^I] = \begin{bmatrix} 1 & 0 & 0 \\ 1 & C_m & C_m^2 \\ C_m & \frac{1}{2} C_m^2 & \frac{1}{3} C_m^3 \end{bmatrix}, [B^I] = \begin{bmatrix} 0 \\ q_m \\ \int_0^{C_m} q_s dC_s \end{bmatrix}$$

**2. Case of  $\phi > V/W$  (region II)**

In this region the original isotherm was approximated by the following linear form

$$q_s^{II} = K_1^{II} C_s + K_o^{II} \tag{12}$$

and superscript II represent the region II. If the equilibrium is an irreversible adsorption, the value of the  $K_1^{II}$  in Eqn(12) should be zero.  $K_1^{II}$  and  $K_o^{II}$  could be ob-

tained by following three methods. The first was Dryden and Kay method [14], and they have approximated to the line  $\overline{QP}$  instead of curve  $\widehat{QP}$  in Figure 2(b), and then

$$K_1^{II} = \frac{q_o - q_m}{C_o - C_m}, \text{ (slope of } \overline{QP}\text{)}$$

$$K_o^{II} = q_m - K_1^{II} C_m \tag{13}$$

The second method was the modified Dryden and Kay method proposed by Hashimoto et al. [4]. They used the centered dashed line  $\overline{AP}$  instead of curve  $\widehat{QP}$  in Figure 2(b), and thus their constants were

$$K_1^{II} = \frac{q_o - q_a}{C_o - C_a}, \text{ (slope of } \overline{AP}\text{)}$$

$$K_o^{II} = q_o - K_1^{II} C_o \tag{14}$$

The point A is arbitrary, and above relations are reduced to the original Dryden and Kay method when the point A comes to point Q.

The third one was proposed in the present work, and the following two conditions were applied.

$$i) \quad q_s^{II}(C_m) = q_s(C_m) = q_m \tag{15}$$

$$ii) \quad \int_{C_m}^{C_o} q_s^{II} dC_s = \int_{C_m}^{C_o} q_s dC_s \text{ (equal area)} \tag{16}$$

Eqn(15) represented the condition that the original isotherm and the approximated isotherm pass to the equilibrium point Q in Figure 2(b), and Eqn(16) was unique in this method and it represented that the area under the curve  $\widehat{QP}$  and the dashed line  $\overline{QP'}$  are same in the operating region,  $C_m < C < C_o$ , as the third condition for region I. Then the following relation was ob-

tained from Eqn(12), (15) and (16)

$$[K^{II}] = [A^{II}]^{-1} [B^{II}] \quad (17)$$

where

$$[K^{II}] = \begin{bmatrix} K_o^{II} \\ K_i^{II} \end{bmatrix}, [A^{II}] = \begin{bmatrix} 1 & C_m \\ (C_o - C_m) & \frac{1}{2} (C_o^2 - C_m^2) \end{bmatrix},$$

$$[B^{II}] = \begin{bmatrix} q_m \\ \int_{C_m}^{C_o} q_s dC_s \end{bmatrix}$$

$K_2^{II}$  is the slope of the dashed line  $\overline{QP'}$  in Figure 2(b). Above three methods coincide with each others when the original isotherm is linear. Since the original isotherm and operating line intersects at point Q, the following relation should be satisfied,

$$q_s(C_m) = \frac{V(C_o - C_m)}{W} \quad (18)$$

and  $Q(C_m, q_m)$  is easily obtained by Newton-Raphson method. The analytical solutions obtained with the approximated isotherm in each region were given as Eqn(19) and Eqn(20) in Table 1. When the external mass transfer resistances are neglected, Eqn(20) can be directly used because the concentrations of fluid phase at the particle surface at the time are always in the region II.

The effect of the parameter  $\phi$  on the fluid phase concentration at the particle surface was shown in

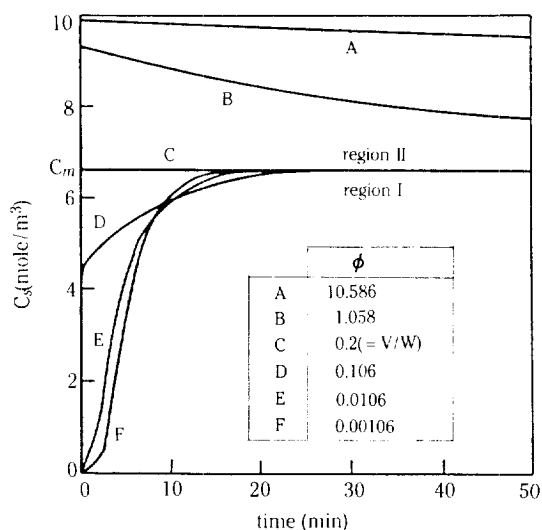


**Fig. 3. Effect of the  $\phi$  on the surface fluid phase concentration ( $k_f = 1 \times 10^{-4}$  m/min,  $V/W = 0.2$  m<sup>3</sup>/kg,  $C_o = 10$  mole/m<sup>3</sup>).**

Figure 3. In the region II  $C_s$  is in  $C_m < C_s < C_o$ , and in the region I  $C_s$  is in  $0 < C_s < C_m$  during all run time. It confirmed the fact that the available isotherm can be divided to two regions, and also it indicated that the time constant line during the whole run time can not jump across the another region at constant  $\phi$ . These

**Table 1. Analytical solution using approximated isotherm**

(A) REGION I ( $\phi < V/W$ )	(B) REGION II ( $\phi > V/W$ )
$\frac{(X - g_1)^{g_1}}{(X - g_2)^{g_2}} = \frac{(X_o - g_1)^{g_1}}{(X_o - g_2)^{g_2}} \exp(-g_3 t) \quad (19)$	$C = [g_2 + (g_1 C_o - g_2) \exp(-g_1 t)] / g_1 \quad (20)$
<p>where</p> $g_1 + g_2 = \left( \frac{V/W - \phi}{K_2^I} \right)$ $g_1 g_2 = - \left[ \frac{(K_1^I + \phi)^2}{(2K_2^I)^2} + \frac{(K_1^I + \phi)(V/W - \phi)}{2(K_1^I)^2} + \frac{(V/W)C_o}{K_2^I} \right], \quad g_1 > g_2$ $g_3 = \frac{3Wk_f}{2RV\rho_p} (g_1 - g_2)$ $X_o = \left[ \frac{(K_1^I + \phi)^2}{(2K_2^I)^2} + \frac{\phi C_o}{K_2^I} \right]^{0.5}$ $X = \left[ \frac{(K_1^I + \phi)^2}{(2K_2^I)^2} + \frac{VC_o}{WK_2^I} - \frac{(V/W - \phi)C}{K_2^I} \right]^{0.5}$	<p>where</p> $g_1 = \frac{3W}{RV} \left( K_1^{II} + \frac{V}{W} \right) \left( \frac{k_s \phi}{K_1^{II} + \phi} \right)$ $g_2 = \frac{3W}{RV} \left( \frac{VC_o}{W} - K_o^{II} \right) \left( \frac{k_s \phi}{K_1^{II} + \phi} \right)$
$\phi \rightarrow 0$ ; external diffusion control	$\phi \rightarrow \infty$ ; internal diffusion control

results were brought about the assumption that the system parameters are independent of time.

**RESULTS AND DISCUSSION**

The adsorption rates of m-cresol, quinoline and 1-naphthol on porous silica gel were measured in a finite bath. Experimental procedures were given elsewhere [15]. The equilibrium data were described by the following equations within an average deviations of 2% ;

m-cresol

$$q_s = \frac{0.118C_s^{0.660}}{1+0.090C_s^{0.660}-0.600C_s^{0.140}} \quad (21)$$

quinoline

$$q_s = \frac{0.524C_s^{0.146}}{1+0.549C_s^{0.146}-0.521C_s^{0.157}} \quad (22)$$

1-naphthol

$$q_s = \frac{1.128C_s}{1+4.692C_s} \left(1 + \frac{0.555C_s}{1+0.148C_s}\right) \quad (23)$$

The isotherm for m-cresol and quinoline was represented by the generalized Toth's and for 1-naphthol the superimposed two-site Langmuir model.

The parameters of the system used were

$$V=7.5 \times 10^{-4} \text{m}^3, R=3.25 \times 10^{-5} \text{m}, \rho_p=614 \text{kg/m}^3$$

$$k_f=9.439 \times 10^{-3} \text{m/min for m-cresol}$$

$$k_f=8.605 \times 10^{-3} \text{m/min for quinoline}$$

$$k_f=6.619 \times 10^{-3} \text{m/min for 1-naphthol}$$

The values of external mass transfer coefficient were

**Table 2. Intraparticle mass transfer coefficient obtained for each run**

RUN	(mole/m <sup>3</sup> ) C <sub>o</sub>	(g) W	k <sub>s</sub> × 10 <sup>6</sup> (m/min)		
			m-cresol	quinoline	1-naphthol
1	5	3.750	-	-	5.646
2	5	5.625	-	-	5.781
3	9	3.750	3.084	5.211	5.682
4	9	5.625	3.844	5.267	6.024
5	15	3.750	3.753	5.471	7.317
6	15	5.625	3.828	5.312	7.583
7	20	3.750	3.979	6.109	7.817
8	20	5.625	4.184	6.572	8.207
9	25	3.750	6.280	9.191	-
10	25	5.625	5.927	8.851	-
11	30	3.750	8.337	9.784	-
12	30	5.625	8.055	10.144	-

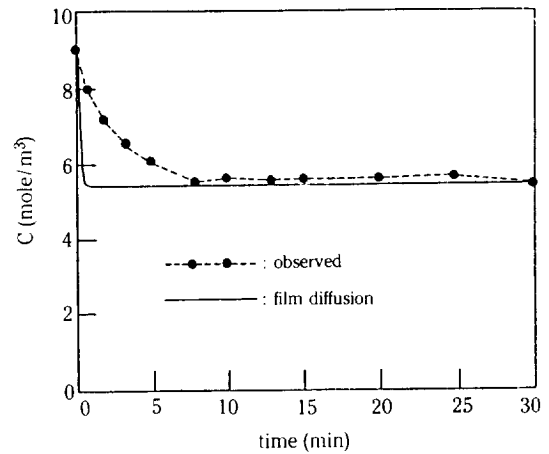


**Fig. 4. Concentration curve of m-cresol.**

determined by the empirical equation(16).

The experimental data for Run 3 of m-cresol in Table 2 was compared with the film diffusion model in Figure 4. The concentration curve for the model was reached instantaneously to equilibrium state. It meant that film diffusion resistances was small as negligible. Similar tendency was obtained for quinoline and 1-naphthol. Accordingly, the present experimental conditions should be in region II. Thus the theoretical concentration curves in this work were calculated by using Eqn(20) in Table 1.

On the other hand, the operating range for the region II(from C<sub>m</sub> to C<sub>o</sub>), i.e., the degree of curvature of available isotherm, varies with C<sub>o</sub> and V/W. When the curvature of available isotherm is very large, the deviations between original nonlinear isotherm and approximated isotherm are also large. Hence the approximate method requires a proper combination of C<sub>o</sub> and V/W to be used within an allowable error. Accordingly, the equilibrium factor, F, defined as Eqn(24), was introduced to express the degree of linearity of available isotherm in the region II.

$$F(C_o, V/W) = \left(\frac{q_o - q_h}{C_o - C_h}\right) / \left(\frac{q_o - q_m}{C_o - C_m}\right) \quad (24)$$

Figure 5 shows that F is a function of the C<sub>o</sub> and V/W. Point H on this figure was selected to middle point for the operating region, i.e. C<sub>h</sub> = C<sub>m</sub> + (C<sub>o</sub> - C<sub>m</sub>)/2. The criteria for linear, favorable and unfavorable of the isotherm are, respectively F = 1, F < 1 and F > 1. When F approaches one, the accuracies of the approximate method increase.

The concentration curve for m-cresol calculated with the nonlinear isotherm was compared with those for the approximated linear isotherm in Figure 6(a) and 6(b). For the modified Dryden and Kay method in these figures, the point A in Figure 2(b) was selected to

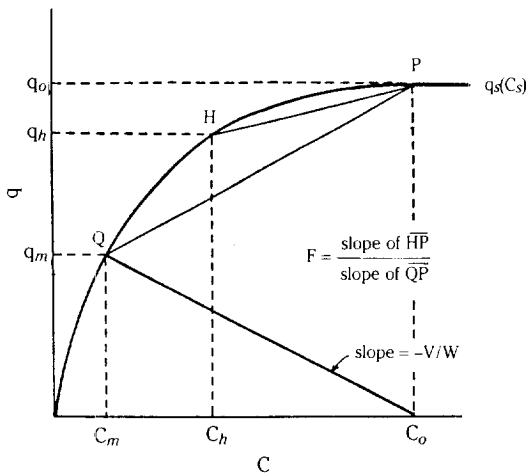


Fig. 5. Schematic diagram for definition of the equilibrium factor(F).

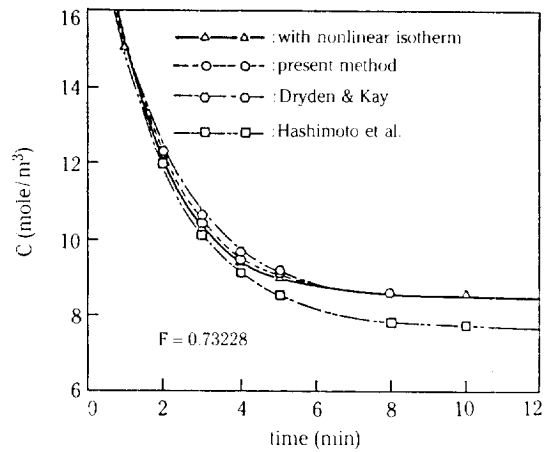


Fig. 6(b). Comparison between concentration curves calculated with nonlinear and approximated linear isotherm at  $F = 0.73228$ .

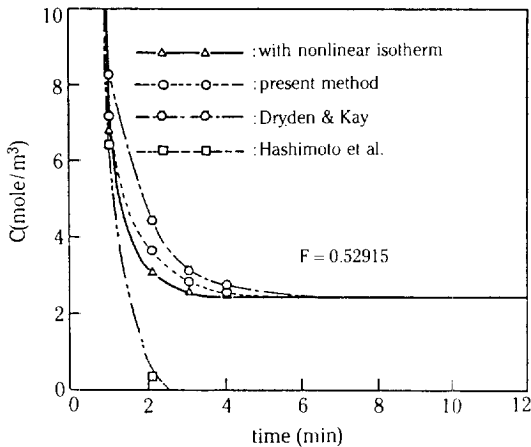


Fig. 6(a). Comparison between concentration curves calculated with nonlinear and approximated linear isotherm at  $F = 0.52915$ .

the half point of the operating region. Comparison of these two figures showed that the deviations of concentration curve calculated with the nonlinear isotherm from those with the approximated isotherm were smaller at higher values of  $F$ . It was due to the fact that the linearity of isotherm was increased with  $F$ . Also the method proposed in present work had less deviations than the others.

For comparing each method for region II, the average percent error(Er) was defined as

$$Er = \frac{1}{N_c} \sum \left| \frac{C_{ALI} - C_{NI}}{C_{ALI}} \right| \times 100 (\%) \quad (25)$$

where  $N_c$  was the number of calculated points, and

$C_{ALI}$  and  $C_{NI}$  represented the concentration of the fluid phase calculated with the approximated linear isotherm and the original nonlinear isotherm, respectively. Figure 7 showed the effects of the  $F$  on Er of quinoline. Er was reduced with increasing of  $F$  and was exactly zero in case  $F = 1$ . Also the present method had the smallest error at fixed  $F$ , i.e. it involved wider range of the  $F$  than the others at same allowable error range. It indicated that the present method had more versatility to the selection of  $C_o$  and  $V/W$  and it was more reliable than the other methods. For each solute the ranges of  $F$  obtained under the present experimental conditions were

$$0.83131 < F < 0.90586 \text{ for m-cresol}$$

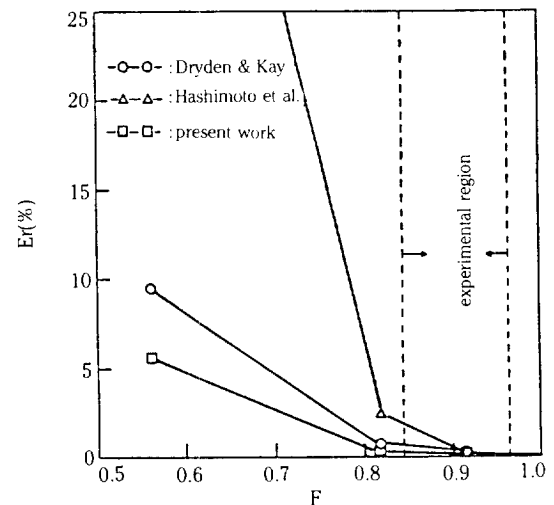


Fig. 7. Effect of  $F$  on Er of the quinoline.

**Table 3. Comparison between slope of time constant line ( $\phi$ ) and slope of operating line (V/W) for all run.**

RUN	(mole/m <sup>3</sup> ) C <sub>o</sub>	(m <sup>3</sup> /kg) V/W	$\phi$ (m <sup>3</sup> /kg)		
			m-cresol	Quinoline	1-naphthol
1	5	0.200	-	-	1.91
2	5	0.133	-	-	1.87
3	9	0.200	4.99	2.69	1.90
4	9	0.133	4.00	2.66	1.79
5	15	0.200	4.10	2.56	1.47
6	15	0.133	4.02	2.64	1.42
7	20	0.200	3.93	2.29	1.38
8	20	0.133	3.67	2.13	1.31
9	25	0.200	2.45	1.53	-
10	25	0.133	2.59	1.58	-
11	30	0.200	1.84	1.43	-
12	30	0.133	1.91	1.38	-

$$0.84661 < F < 0.96915 \quad \text{for quinoline}$$

$$0.83000 < F < 0.91237 \quad \text{for 1-naphthol}$$

Errors for each solute in the above range of F were within about 2%, and it gave a good reason for usefulness of the present approximation.

The values of  $k_s$  obtained by comparing the theoretical curve and experimental data were given in Table 2. These values were increased with  $C_o$ . It can be explained that mass transfer rate into the particle is high in the system with large  $C_o$  since the average bonding energy between solute and particle surface is decreased with  $C_o$  [17].

To check the present experimental conditions was in region II, values of the  $\phi$  for all runs were calculated, and the results were given in Table 3. The values of  $\phi$  shown were larger than these of V/W for all runs. Thus the present experimental conditions were well inside of region II.

### CONCLUSIONS

In general the intraparticle mass transfer coefficient is not constant but it can be treated as constant by taking as average value for the operating region. Then the slope of the constant time line is independent of time. This property allowed that the region of available isotherm can be divided into two parts by the operating conditions. Hence the original nonlinear isotherm with the restriction of equal area under isotherms was approximated by the quadratic form in region I where the slope of the constant time line is less than that of the operating line, and by the linear form in region II

where the slope of the constant time line is larger than that of the operating line. The present experimental operating conditions were in region II, and the present work appeared to be a good simplified method to obtain approximate solution of model equation and especially it was more reliable method than the other methods applied for region II such as Dryden and Kay and modified Dryden and Kay.

### NOMENCLATURE

- C : fluid phase concentration [mole/m<sup>3</sup>]  
 C<sub>m</sub> : fluid phase concentration at equilibrium [mole/m<sup>3</sup>]  
 C<sub>s</sub> : fluid phase concentration at the particle surface [mole/m<sup>3</sup>]  
 Er : average percent error [%]  
 F : equilibrium factor [-]  
 K : equilibrium parameters  
 k<sub>f</sub> : external mass transfer coefficient [m/min]  
 k<sub>s</sub> : intraparticle mass transfer coefficients [m/min]  
 N<sub>c</sub> : number of calculated points [-]  
 q : average solid phase concentration [mole/kg]  
 q<sub>m</sub> : solid phase concentration at equilibrium [mole/kg]  
 q<sub>s</sub> : solid phase concentration at the particle surface [mole/kg]  
 R : mean particle radius [m]  
 t : time [min]  
 V : volume of solution [m<sup>3</sup>]  
 W : weight of adsorbent [kg]

### Greek Letters

- $\rho_p$  : particle density [kg/m<sup>3</sup>]  
 $\phi$  :  $k_f/k_s \rho_p$  [m<sup>3</sup>/kg]

### REFERENCES

- Liapis, A.L. and Lippin, D.W.T.: *Chem. Eng. Sci.*, **32**, 619 (1977).
- Spahn, H. and Schlünder, E.U.: *Chem. Eng. Sci.*, **30**, 529 (1975).
- Costa, C. and Rodrigues, A.: *Chem. Eng. Sci.*, **40**, 983 (1985).
- Hashimoto, K., Miura, K., and Nagata, S.: *J. Chem. Eng. Japan*, **8**, 367 (1975).
- Huang, T.C. and Li, K.Y.: *Ind. Eng. Chem. Fundam.*, **12**, 50 (1973).
- McKay, G.: *J. Chem. Tech. Biotechnol.*, **34A**, 294 (1984a).
- McKay, G.: *AIChE J.*, **31**, 335 (1985).
- Tien, C.: *Can. J. Chem. Eng.*, 25 (1960).
- Moon, H. and Lee, W.K.: *J. Colloid Interface Sci.*, **96**, 162 (1983).

10. Glueckauf, F. and Coates, J.I.: *Trans. Faraday Soc.*, **51**, 1315 (1947).
11. Jury, S.H.: *AIChE J.*, **13**, 1124 (1967).
12. McKay, G.: *AIChE J.*, **30**, 692 (1984b).
13. Miller, C.O.M. and Clump, C.W.: *AIChE J.*, **16**, 169 (1970).
14. Dryden, C.E. and Kay, W.B.: *Ind. Eng. Chem.*, **46**, 2294 (1954).
15. Moon, J.K. and Lee, W.K.: "Equilibrium adsorption and mass transfer of aromatics onto the silica gel", M.S. Thesis, KAIST, 1987.
16. Mistic, D.M., Sudo, Y., Suzuki, M., and Kawazoe, K.: *J. Chem. Eng. Japan*, **15**, 67 (1982).
17. Fritz, W., Merk, W., and Schlünder, E.U.: *Chem. Eng. Sci.*, **36**, 731 (1981).